

Accounts

Reversible O_2-Binding and Activation with Dicopper and Diiron Complexes Stabilized by Various Hexapyridine Ligands. Stability, Modulation, and Flexibility of the Dinuclear Structure as Key Aspects for the Dimetal/O_2 Chemistry

Masahito Kodera* **and Koji Kano**

Department of Molecular Science and Technology, Doshisha University, Kyotanabe, Kyoto 610-0321

Received July 25, 2006; E-mail: mkodera@mail.doshisha.ac.jp

Reversible O_2-binding and activation have been studied using dicopper and diiron complexes of various hexapyridine ligands as functional models of hemocyanin (Hc) and soluble methane monooxygenase (sMMO), respectively. Dicopper(I) complexes of sterically hindered hexapyridine ligands react with O_2 to form μ-η^2:η^2-peroxo–dicopper(II) complexes stable at room temperature, which release O_2 to attain reversible O_2-binding. When a sterically hindered hexapyridine ligand methylated at the bridgehead positions is used, the O_2-release becomes easier, and reversibility is greatly improved. Detailed structural studies of Cu^I and Cu^{II} complexes of sterically hindered tripyridine ligands showed that the bridgehead alkyl group causes a pyridine shift leading to structural modulation of the copper complexes. A hexapyridine ligand can be used to form a thermally stable peroxo–diiron(III) complex, which can oxygenate hydrocarbons upon addition of acid chloride/DMF. Diiron(III) complexes of a bis-tpa type hexapyridine ligand catalyze epoxidation of various alkenes with H_2O_2. A peroxo–diiron(III) complex is detected as an intermediate. Detailed isotope-labeling experiments showed that the peroxo intermediate is converted to dioxo–μ-oxo–diiron(IV) complex, and that three oxygen atoms of the active species scramble with each other. Stable dinuclear structure, structural modulation, and structural flexibility, which may be from the hexapyridine ligands, play key roles in reversible O_2-binding and activation by the dicopper and diiron complexes.

Introduction

It is a great challenge in chemistry to synthesize simple model compounds capable of reproducing biological functions, which are useful not only for understanding biological mechanisms but also for developing practical bio-inspired molecules.[1–3] Reversible O_2-binding and activation are the key reactions in O_2-transport and oxygenation of various substrates, which are biologically essential functions mostly performed by heme proteins and non-heme metalloproteins.[4,5] Thus, so far enormous numbers of heme and non-heme model compounds have been developed, and structural, spectroscopic, kinetic, and thermodynamic studies have made a great progress in understanding of biologically related metal dioxygen chemistry.

Over the last two decades, excellent model compounds of non-heme systems have been developed.[6–15] On such system that have been modeled extensively is hemocyanins (Hc), which is type III copper proteins that transport O_2 molecule in mollusks and arthropods.[16] Reversible O_2-binding involving Hc is shown in Scheme 1. Karlin and some copper coordination chemists innovated model studies of Hc with dinuclear copper complexes with mononucleating ligands, for example, tpa, tepa, and their derivatives, and dinucleating ligands, e.g., XYL, Nn, and their derivatives (see Chart 1).[6] From one of the most important studies in bioinorganic chemistry, thermally stable μ-η^2:η^2-peroxo–dicopper(II) complexes (μ-η^2:η^2-Cu_2O_2) of sterically hindered hydrotris(pyrazol-1-yl)borato ligands (HB(3,5-R_2-pz)$_3$, R = Me, *iso*-Pro, and various alkyl groups, see Chart 1) were reported by Kitajima[7] at the end of the 1980's as real structural models that precisely predicted the structure of oxyhemocyanin (oxyHc) several years before the crystal structure of oxyHc[16] was determined. Typical ligands used for peroxo–dicopper complexes are shown in Chart 1. In spite of these excellent studies, it is still difficult to make a real functional model of oxyHc, a thermally stable μ-η^2:η^2-Cu_2O_2 complex which can bind an O_2 molecule reversibly at around room temperature.

Soluble methane monooxygenases (sMMO) are non-heme diiron enzymes that catalyzes the conversion of methane to methanol in methylotrophs.[17,18] It has been postulated that the diiron(II) center binds an O_2 molecule to form a peroxo–diiron(III) intermediate P via two transient intermediates O and P*, and P is converted to an active species Q that oxidizes

Published on the web April 13, 2007; doi:10.1246/bcsj.80.662

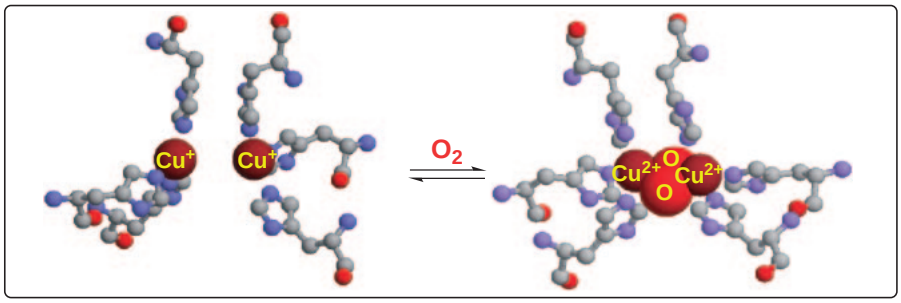

Cu···Cu 4.6 Å
trigonal planar

Cu···Cu 3.6 Å
square pyramid

Scheme 1. Reversible O_2-binding of hemocyanin.

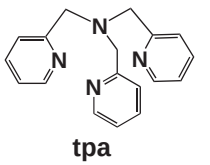

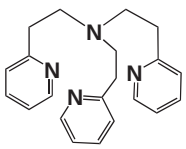

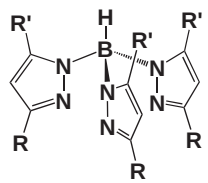

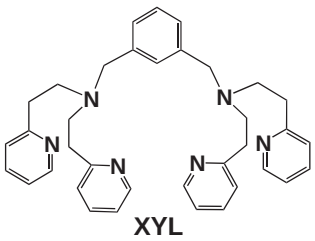

Chart 1.

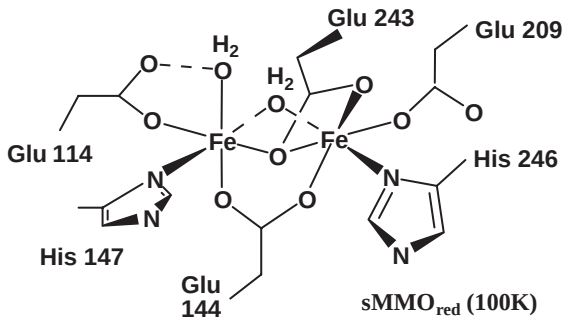

Crystal Structure of the Active Site of sMMO[94]

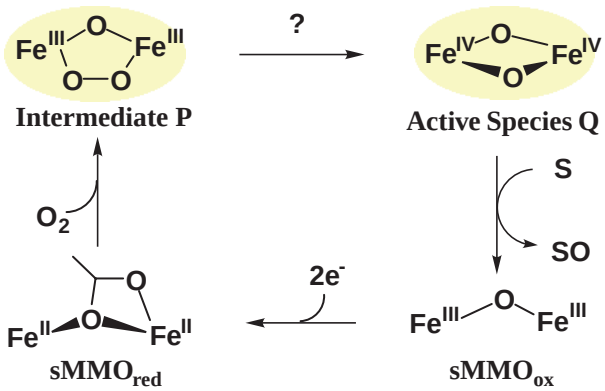

Scheme 2. Active site structure and plausible mechanism for O_2-activation of sMMO.

methane to methanol.[19,20] A plausible mechanism for the O_2-activation is shown in Scheme 2. The active species Q was detected as a transient species by Mössbauer and EXAFS spectra using a rapid freeze-quench technique for the reaction of O_2 with diiron(II) hydroxylase (MMOH) and component B (MMOB).[21–25] However, mechanistic studies employing native enzymes are still difficult due to the instability of P and Q, and the mechanism for the conversion of P to Q remains unknown. Several peroxo–diiron(III) complexes have been synthesized as models of the intermediate P, and peroxo–diiron(III) complexes with sterically hindered ligands, such as Ph–bipm,[26] HB(3,5-*i*Pr$_2$pz)$_3$,[27] and Me$_4$–tpdp,[28] were structurally characterized. The chemical structures of the ligands are shown in Chart 2. Que and Dong proposed that the Q is a bis[(μ-oxo)-iron(IV)] complex by using di-μ-oxodiiron complexes supported by sterically hindered derivatives of tpa and mep type ligands (see Chart 2) as model compounds.[29] Thus, peroxo–diiron(III) and high valent oxo–diiron complexes are useful as models of P and Q, respectively. Recently, mononuclear oxo–iron(IV) complexes were synthesized and fully charac-

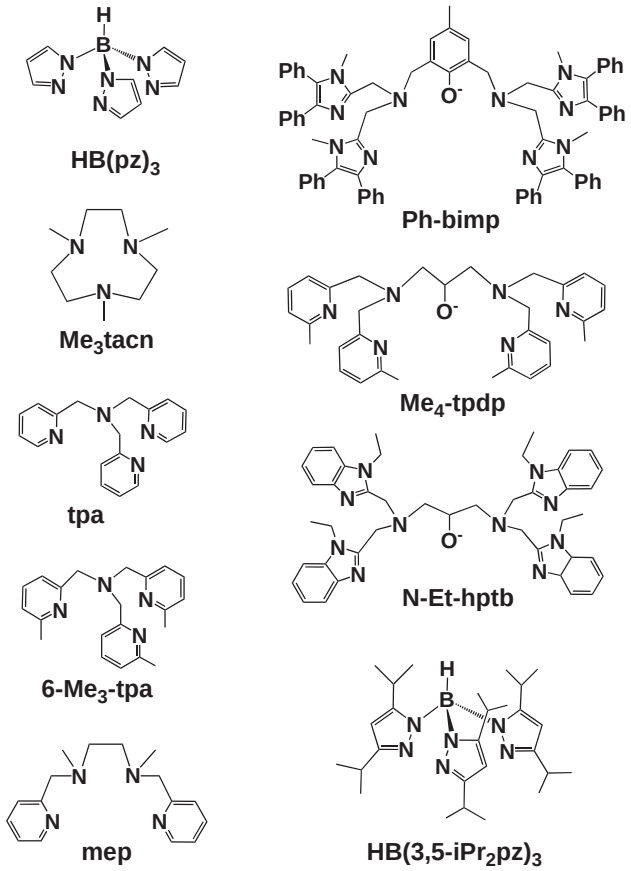

Chart 2.

terized with X-ray crystallography, spectroscopy, and reactivity,[30–32] but oxo–diiron(IV) complexes have not been fully investigated due to their instability. Ligands used for these model compounds are shown in Chart 2. A fully functional model of sMMO, which efficiently catalyzes substrate oxygenation via the conversion of the peroxo–diiron(III) species to the oxo–diiron(IV) species, is the final goal of the model studies.

In this account, we introduce our recent studies on reversible O_2-binding by dicopper complexes and O_2-activation by diiron complexes, in which a series of hexapyridne ligands, 1,2-bis[6-di(2-pyridyl)methyl-2-pyridyl]ethane (hexpy),[33] 1,2-bis[2-di(6-methyl-2-pyridyl)methyl-6-pyridyl]ethane (H6M4h),[34] and 1,2-bis[2-(1,1-di(6-methyl-2-pyridyl)ethyl)-6-pyridyl]ethane (M6M4h),[35] and a bis-tpa type hexapyridine ligand, 1,2-bis[2-[di(2-pyridylmethyl)aminomethyl]-6-pyridyl]ethane (6-hpa)[36] have been developed. The chemical structures of these ligands are shown in Chart 3. In the first three ligands, two tripyridylmethane derivatives are attached at both sides of a $–CH_2CH_2–$ tether, and in the last ligand, two tpa moieties are attached in the same manner. A 1,2-bis(2-pyridyl)ethane group is included in these ligands as a common moiety, and it plays an essential role in stabilizing the dinuclear structures and in optimizing the distance between the two metal ions.[37] Stabilization, structural modulation, and structural flexibility of the dinuclear structure with the hexapyridine ligands play key roles in reversible O_2-binding and activation by the dicopper and diiron complexes.

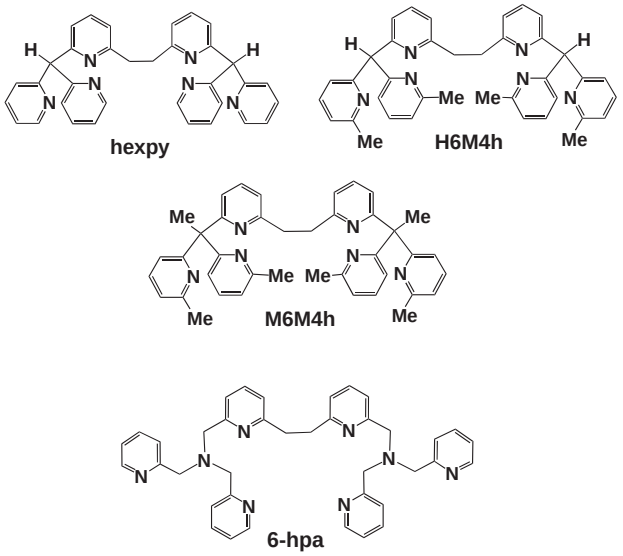

Chart 3.

1. Reversible O_2-Binding with Thermally Stable μ-η^2:η^2-Peroxo–Dicopper(II) Complexes

The first example of a thermally stable μ-η^2:η^2-Cu_2O_2 complex was reported by Kitajima as mentioned above.[7] After that, several μ-η^2:η^2-Cu_2O_2 complexes with various ligands have been reported,[38–43] but most of them are thermally unstable. Karlin et al. reported O_2-binding and O_2/CO cycle involving dicopper(I) complexes with dinucleating tetrapyridine ligands Nn[44] (see Chart 1), but thermal stability of the peroxo complexes is not good enough to carry out reversible binding at room temperature. The difficulty in reversible O_2-binding is mainly due to low thermal stability of the peroxo complexes. We have solved the problem by using sterically hindered hexapyridine ligands that can stabilize not only the dinuclear structure but also highly reactive μ-η^2:η^2-Cu_2O_2 moiety.[34] In this section, our synthetic efforts to obtain thermally stable μ-η^2:η^2-Cu_2O_2 complexes and to achieve reversible O_2-binding is presented.

A variety of dinucleating ligands has been developed so far, most of which have an endogenous bridging group to stabilize the dinuclear metal complexes.[45] Such ligands formed various dinuclear metal peroxo complexes but not the μ-η^2:η^2-Cu_2O_2 complex. The dinucleating ligands that have an endogenous bridging group are not suitable for preparing μ-η^2:η^2-Cu_2O_2 complexes because no bridging ligand other than a peroxo ligand is involved in the μ-η^2:η^2-Cu_2O_2 complex. So, in the beginning of this study, we designed a hexapyridine ligand (hexpy) (see Chart 3), that has two tripyridylmethane moieties connected by a $–CH_2CH_2–$ tether, which does not have any endogenous bridging group.[46] The hexpy ligand binds two metal ions at the tridentate donors to stabilize dimetal complexes not only in the solid state but also in solution.[47] The crystal structure of di-μ-hydroxo–dicopper(II) complex of the hexpy ligand is shown in Fig. 1. The hexpy ligand encapsulates the dicopper core to stabilize it.

Kitajima et al. reported that the μ-η^2:η^2-Cu_2O_2 complex of $HB(3,5\text{-}R_2\text{-}pz)_3$ is prepared upon reaction of the di-μ-hydroxo–dicopper(II) complex with H_2O_2.[48] Accordingly, with

the aim to obtain a μ-η^2:η^2-Cu_2O_2 complex, a di-μ-hydroxo–dicopper(II) complex of hexpy ligand was reacted with H_2O_2 in MeCN/CH_2Cl_2 (1:9, v/v) at a low temperature.[46] The solution turned dark purple, suggesting the formation of the μ-η^2:η^2-Cu_2O_2 complex. However, detailed spectral studies clearly showed generation of two different species, μ-hydrogenperoxo-μ-hydroxo–dicopper(II) and μ-hydroxo-μ-superoxido–dicopper(II) complexes.[46] The structures of these species are shown in Scheme 3.

This system efficiently catalyzes oxidation of 2,4-di-*tert*-butylphenol (DBP) to 3,3′,5,5′-tetra-*tert*-butyl-2,2′-dihydroxybiphenyl (see Scheme 4), and kinetic studies for the reaction provided some insight into the mechanism for the generation of the superoxido and hydrogenperoxo species.[47] The second-order rate constant (k_2) for the DBP oxidation with this system is 17 M^{-1} s^{-1}, which is 3-times larger than 5.3 M^{-1} s^{-1} of the largest k_2 value reported for DBP oxidation by hydrogenperoxo–dicopper(II) complexes.[47,49] This suggested that the actual oxidant is not two species that were detected by spectroscopy and a more reactive species might exist in this reaction system. μ-η^2:η^2-Cu_2O_2 or di-μ-oxo–dicopper(III) complexes is possibly the active species in this system. In the absence of substrate, these species could abstract a H-atom from the hydrogenperoxo species to generate the superoxido species. Thus, the generation of μ-η^2:η^2-Cu_2O_2 complex with the hexpy ligand may occur, though it is too reactive to be detected by spectroscopy. A plausible mechanism for formation of the superoxido species is shown in Scheme 4.

The hexpy ligand forms stable dinuclear complexes but did not stabilize the μ-η^2:η^2-Cu_2O_2 complex, which may be due to no steric hindrance. Thus, it is not suitable for preparing a functional model of Hc that can bind O_2 reversibly. To enhance the thermal stability of μ-η^2:η^2-Cu_2O_2 complex, we synthesized a sterically hindered hexapyridine ligand 1,2-bis[2-(bis(6-methyl-2-pyridyl)methyl)-6-pyridyl]ethane

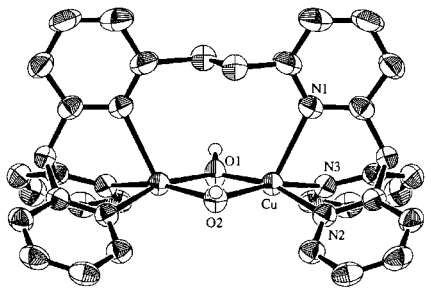

Fig. 1. ORTEP diagram of the cationic portion of $[Cu_2(OH)_2(hexpy)](ClO_4)_2$.

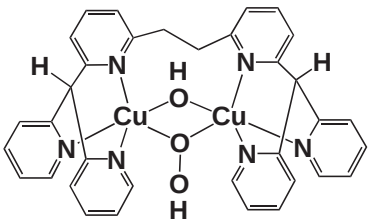

Scheme 3. Proposed chemical structures of hydrogenperoxo– and superoxido–dicopper complexes.

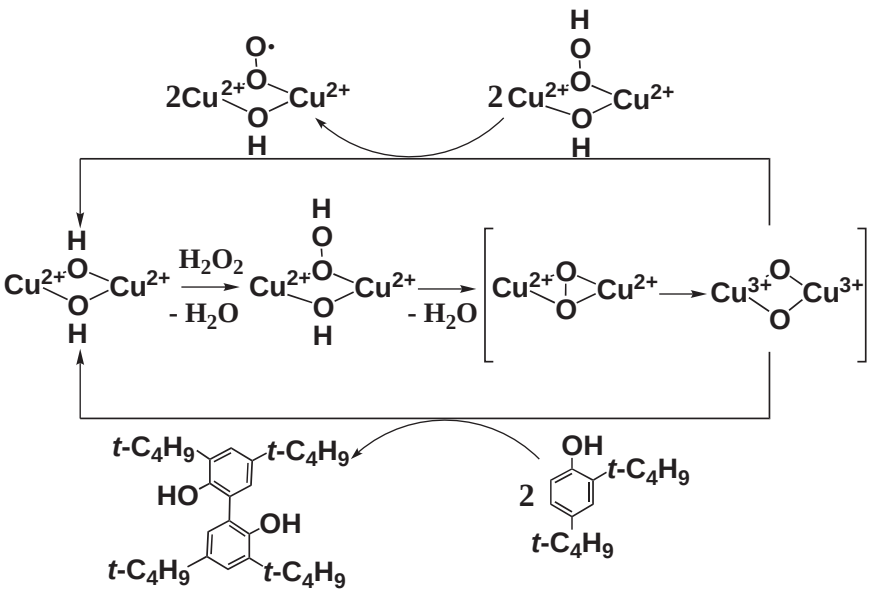

Scheme 4. Proposed mechanism for formation of superoxido–dicopper(II) complex upon reaction of di-μ-hydroxo–dicopper(II) complex with H_2O_2 and oxidation of DBP with this system.

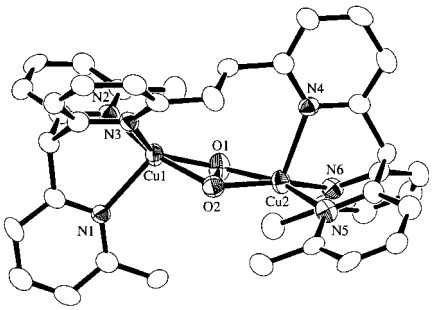

Fig. 2. ORTEP diagram of the cationic portion of μ-η^2:η^2-peroxo–dicopper(II) complexes with sterically hindered hexapyridine ligand $[Cu_2(O_2)(H6M4h)](PF_6)_2$ (**2**-$(PF_6)_2$).

(H6M4h) (see Chart 3), in which four methyl groups are introduced at the 6-positions of the pyridyl groups of the hexpy ligand.[34] A similar method was reported by Suzuki et al., where a 6-methyl group on the pyridine ring was used in Me_4tpdp ligand[50] (see Chart 2) as steric hindrance to stabilize peroxo–diiron(III) complexes against the thermal decomposition. The H6M4h ligand forms a dicopper(I) complex **1**, which reacts with O_2 to afford a thermally stable μ-η^2:η^2-Cu_2O_2 complex **2**.[34] The half-life time of **2** in CH_2Cl_2 at 25 °C is 25.5 h.[34] To our knowledge, this is the most thermally stable μ-η^2:η^2-Cu_2O_2 complex reported so far.

Physicochemical properties of **2** are almost the same as those of oxyHc and related μ-η^2:η^2-Cu_2O_2 complexes.[9] The crystal structure (Fig. 2) shows that **2** has a dicopper(II) unit bridged by a peroxo in the μ-η^2:η^2-mode.[34] The H6M4h ligand stabilizes **2** by encapsulating the μ-η^2:η^2-Cu_2O_2 core with the four 6-methyl groups and the $-CH_2CH_2-$ tether. The tether group also enhances the stability of **2** by holding the two $Cu(py)_3$ moieties at an optimum distance. The Cu···Cu distance 3.477 Å of **2** is slightly shorter than 3.560 Å of μ-η^2:η^2-Cu_2O_2 complex of $HB(3,5\text{-}R_2\text{-}pz)_3$ (R = *iso*-propyl) (**3**). However, the O–O bond length 1.485 Å of **2** is slightly longer than 1.412 Å of **3**. The overall structural features (O_2-bridging mode, bond lengths about Cu_2O_2 core, and anti-configuration of the two axial Cu–N bonds) of **2** are similar to those of oxyHc and **3**. The bond angles about the Cu atoms in **2**, however, are more distorted than those in **3**. The Cu–O_2–Cu of **3** is planar, but that of **2** is slightly bent. The distortion of the copper geometry is shown by a τ value, which varies from 0 for an idealized square pyramidal to 1 for an idealized trigonal bipyramidal. The τ values of **2** (0.44 and 0.16) are much larger than that of **3** (0.02), showing that the copper coordination geometry of **2** is distorted square pyramidal.[34,48]

Reversible O_2-binding occurs with **2**. Under anaerobic conditions O_2 was released in MeCN–CH_2Cl_2 (0.001:3, v/v) to form **1**, and **2** was regenerated by adding O_2 at room temperature.[34] After three cycles of the reversible O_2-binding, the irreversible decomposition of **2** is less than 30%. In the reversible O_2-binding experiments, an excess amount of MeCN was necessary for O_2-release from **2**, and the temperature was increased to 80 °C to accelerate O_2-release. This is the first example of reversible O_2-binding at room temperature via a μ-η^2:η^2-Cu_2O_2 complex. Kitajima et al. reported that μ-η^2:η^2-Cu_2O_2 complexes with $HB(3,5\text{-}R_2\text{-}pz)_3$ release O_2 upon addition of excess amount of MeCN, CO, and $P(Ph)_3$, but the generated Cu^I complexes are too stable to bind O_2.[51] Gorun et al. reported an O_2-binding cycle by using a μ-η^2:η^2-Cu_2O_2 complex with $HB(3\text{-}CF_3\text{-}5\text{-}CH_3\text{-}pz)_3$ (see Chart 1), where the μ-η^2:η^2-Cu_2O_2 complex releases O_2 by dissolving it in acetone to give the Cu^I complex, and the isolated Cu^I complex forms the μ-η^2:η^2-Cu_2O_2 complex upon reaction with O_2 in CH_2Cl_2.[52] However, this cycle is not really reversible O_2-binding because it is not done in one-pot. Thus, **2** is a special example for reversible O_2-binding via μ-η^2:η^2-Cu_2O_2 complex at around room temperatures. The reason why **2** can reproduce O_2-transporting functions of Hc is mainly the high thermal stability of the μ-η^2:η^2-Cu_2O_2 core in solution, which was achieved by using a sterically hindered hexapyridine ligand.

2. Reversible O_2-Binding Greatly Improved by Structural Modulation

Structural modulation of the copper complexes by subtle perturbations of various tridentate and tetradentate ligands have been studied to understand the Cu/O_2 chemistry.[53–55] Karlin et al. reported that the length of the tether groups (methyl or ethyl) in tris(2-pyridylmethyl)amine (tpa) and tris(2-pyridylethyl)amine (tepa) (see Chart 1) had a drastic effect on the Cu^I/O_2 reactivity and recently showed more detailed results with a variety of related ligands.[56–60] Suzuki et al. showed that a 6-Me group on pyridine rings in tpa derivatives drastically affects coordination structures and redox potentials of the copper complexes.[61] Itoh et al. reported that attaching a methyl group to a tether group in tepa derivatives produced unique effects.[62,63] It is well-known that 3,5-bulky alkyl groups of $HB(3,5\text{-}R_2\text{-}pz)_3$ are effective for preventing formation of a bis-ligand monometal complex, and thus the ligands are useful to model both monometal and dimetal active sites of metalloproteins.[64–66]

We found that copper complexes with sterically hindered tripyridine ligands can be structurally modulated by introducing an alkyl group at the bridgehead position of the ligand.[67] We prepared three sterically hindered tripyridine ligands: tris(6-methyl-2-pyridyl)methane (H6M3t),[68] 1,1,1-tris(6-methyl-2-pyridyl)ethane (Me6M3t),[67] and 1,1,1-tris(6-methyl-2-pyridyl)propane (Et6M3t).[67] The chemical structures of H6M3t,

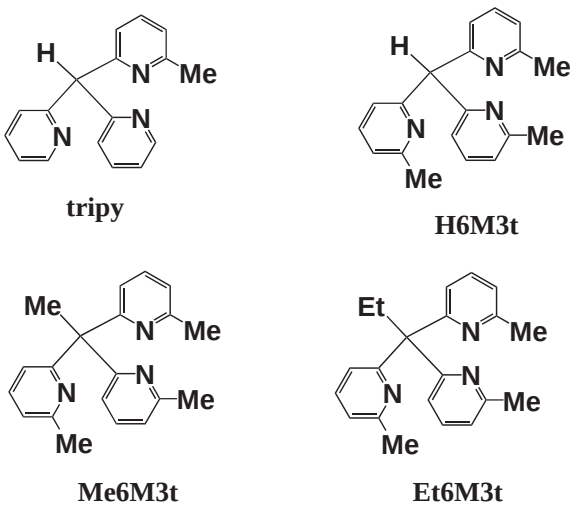

Chart 4.

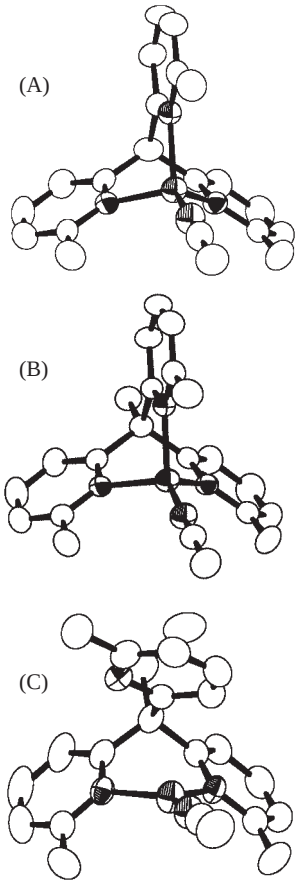

Fig. 3. ORTEP diagrams of the cationic portions of Cu^{I} complexes of (A) H6M3t, (B) Me6M3t, and (C) Et6M3t.

Me6M3t, and Et6M3t are shown in Chart 4. Crystal structures of Cu^{I} complexes with these ligands are shown in Fig. 3, and the pyridine rings in the copper complexes of Me6M3t clearly shift toward the Cu side as compared to those in the copper complexes of H6M3t. This is caused by steric repulsion between the bridgehead methyl group and the 3-H_{py} atoms. We call this "pyridine shift."[67] The pyridine shift between the Cu^{I} complexes of H6M3t and Me6M3t is schematically drawn on the basis of the crystal structures in Scheme 5. The pyridine shift leads to subtle but significant changes in the copper coordination structures. For example, the average Cu–N_{py} bond distance in the Cu^{I} complex of Me6M3t is shorter by 0.022 Å than the comparable distance in the Cu^{I} complex of HL, and the Cu–N_{MeCN} bond distance in the former is longer by 0.017 Å than the comparable distance in the latter. The elongation of the Cu–N_{MeCN} bond distance by the bridgehead methyl group indicates that the pyridine shift may enhance the steric hindrance by the 6-Me groups. The bridgehead ethyl group causes much more drastic structural changes (see Fig. 3). The steric effects of the bridgehead alkyl groups are found not only in the solid state but also in solution. Electronic absorption and ^{1}H NMR spectra of the Cu^{I} complexes are consistently explained by the crystal structures.[67]

By using M6M4h (see Chart 3), which is a sterically hindered hexapyridine ligand methylated at the bridgehead positions, we succeeded in greatly improving the reversibility for the O_2-binding of the μ-η^2:η^2-Cu_2O_2 complex.[35] The M6M4h

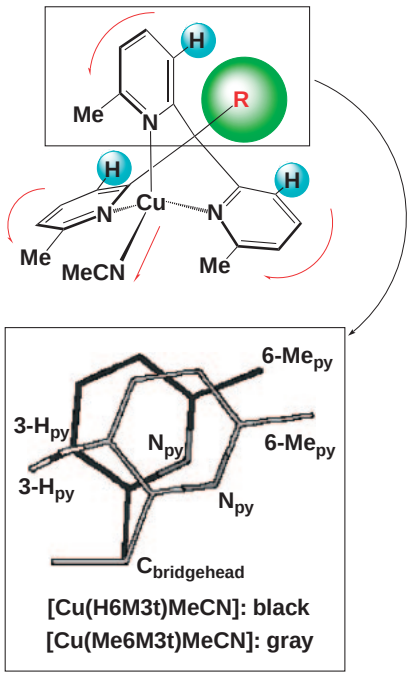

Scheme 5. Pyridine shift schematically shown on the basis of the crystal structures of Cu^{I}–MeCN complexes of H6M3t and Me6M3t ligands.

ligand forms Cu^{I} complexes (**4**-X_2; X = PF_6, CF_3SO_3, and ClO_4). The μ-η^2:η^2-Cu_2O_2 complexes **5**-X_2 were formed by addition of O_2 to the dicopper(I) complexes **4**-X_2 in CH_2Cl_2 and isolated as purple crystals.[35] Reversible binding of O_2 was observed in CH_2Cl_2/acetone (3/0.002) (Fig. 4A), and **5** releases O_2 under Ar and is easily regenerated by replacing the gas phase over the solution with O_2.[35] A small amount of acetone assists the release of O_2 from **5** by coordinating to the Cu^{I} center. Replacement of the O_2 atmosphere with Ar is sufficient to release O_2 from **5**. After three cycles of reversible O_2 binding, the irreversible decomposition of **5** was less than 10%. Thus, the reversible O_2-binding ability of **5** is greatly improved over that of the μ-η^2:η^2-Cu_2O_2 complex of H6M4h.[35] Moreover, we prepared a Cu^{I}–CO complex of M6M4h (**6**-$(PF_6)_2$) and achieved complete reversible O_2/CO binding (Fig. 4B) with a solution of **6** in CH_2Cl_2 at 25 °C without addition of any coordinating solvent and without heating.[35] In this system, **6** is easily converted to **5** by addition of O_2 and regenerated quantitatively by evacuation of O_2 and refilling with CO. After several CO/O_2 cycles, **6** was quantitatively recovered from the solution. Irreversible decomposition of **5** and **6** during the reversible CO/O_2 cycle is negligibly small (see Fig. 4B). The reason for the greatly improved reversibility is the easy release of O_2 from **5**.

The crystal structure of **5**-$(PF_6)_2$ was determined by X-ray analysis, and showed that there are two independent molecules **5a** and **5b** in the crystal, both of which are similar to each other (Fig. 5).[35] Though the overall structure of **5**[35] is similar to that of the μ-η^2:η^2-Cu_2O_2 complex of H6M4h,[34] in the former, steric repulsion between the bridgehead methyl groups and 3-py H atoms causes a pyridine shift,[67] leading to significant structural differences. The pyridine shift enhances the steric hindrance of the 6-Me groups and thus causes an elongation

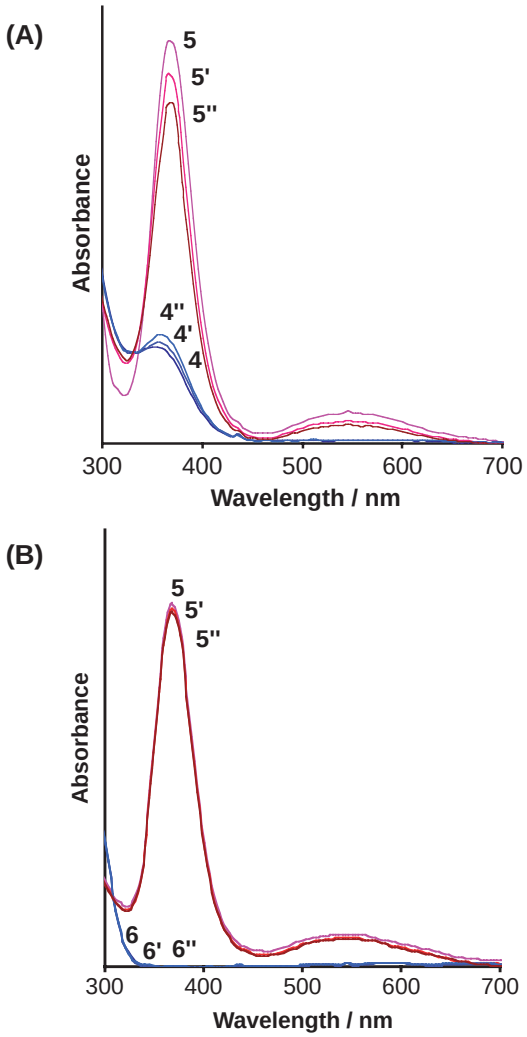

Fig. 4. (A) Reversible O_2 binding by **4**-$(PF_6)_2$ in CH_2Cl_2/acetone (3/0.002, v/v). A solution of **4**-$(PF_6)_2$ was oxygenated under O_2 to give **5**-$(PF_6)_2$, and **4**-$(PF_6)_2$ was regenerated from **5**-$(PF_6)_2$ under Ar. Three cycles are shown. (B) Reversible CO/O_2 cycle by **6**-$(PF_6)_2$ in CH_2Cl_2. A solution of **6**-$(PF_6)_2$ was oxygenated under O_2 at room temperature to form **5**-$(PF_6)_2$, and **6**-$(PF_6)_2$ was regenerated from **5**-$(PF_6)_2$ under CO. Three cycles are shown.

of the Cu–O and Cu···Cu distances in **5**. The average Cu–O bond lengths of 1.922 and 1.918 Å and Cu···Cu separations of 3.523 and 3.516 Å for **5a** and **5b**, respectively, are larger than those of 1.910 and 3.477 Å, respectively, for the μ-η^2:η^2-Cu_2O_2 complex of H6M4h. The Cu–O bond of **5** is the longest in structurally characterized μ-η^2:η^2-Cu_2O_2 complexes (1.89–1.915 Å).[35] The μ-η^2:η^2-Cu_2O_2 core of **5** is more planar than that of the μ-η^2:η^2-Cu_2O_2 complex of H6M4h; the Cu–O–O′–Cu′ dihedral angles of 168.22 and 168.45° of **5a** and **5b**, respectively, are closer to 180° than 163.3° of the μ-η^2:η^2-Cu_2O_2 complex of H6M4h. The more planar μ-η^2:η^2-Cu_2O_2 core in **5** may be due to elongation of the Cu···Cu distance. The copper coordination geometry of **5** is less distorted from square pyramidal than that of the μ-η^2:η^2-Cu_2O_2 complex of H6M4h; the τ values of 0.00 and 0.37 for **5a** and 0.00 and 0.38 for **5b** are smaller than 0.16 and 0.44 for the μ-η^2:η^2-Cu_2O_2 complex of H6M4h.[34,35] These data suggest that the easy release of O_2 from **5** is due to the elongation of the Cu–O bond and the Cu···Cu distance, and O_2-release is not inhibited by the planar structure of the Cu_2O_2 core and by the less distorted copper coordination geometry.

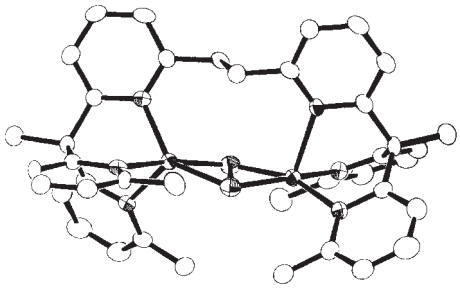

(5a) Cu-N: 2.053, Cu-O: 1.922, Cu···Cu: 3.523
τ: 0.00 (Cu1), 0.37 (Cu2)

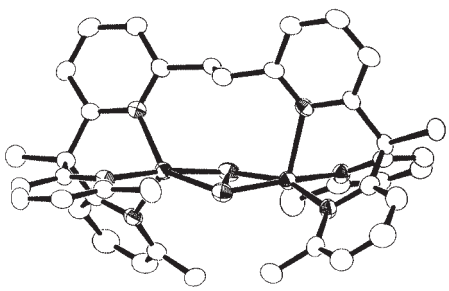

(5b) Cu-N: 2.051, Cu-O: 1.918, Cu···Cu: 3.516
τ: 0.00 (Cu1), 0.38 (Cu2)

Fig. 5. ORTEP diagrams of the cationic portion of μ-η^2:η^2-peroxo–dicopper(II) complex with sterically hindered hexapyridine ligand methylated at the bridgehead positions $[Cu_2(O_2)(M6M4h)](PF_6)_2$ (**5**-$(PF_6)_2$). The X-ray structure analysis of **5**-$(PF_6)_2$ revealed two independent molecules **5a** and **5b**, which are similar to each other.

The resonance Raman spectrum of **5**, obtained with excitation at 514.5 nm, has a strong band at 765 cm^{-1}, which shifts to 724 cm^{-1} on labeling with ^{18}O and is assigned to the O–O stretch of a bound peroxo in a μ-η^2:η^2-mode on the basis of its frequency and isotope shift (41 cm^{-1}).[35] Solomon et al. reported that the O–O stretch moves to higher energy as the μ-η^2:η^2-Cu_2O_2 core becomes more bent and that the Cu···Cu distance shortens.[69] In contrast, the ν_{O-O} band (765 cm^{-1}) of **5** is at higher wave number than that of the μ-η^2:η^2-Cu_2O_2 complex of H6M4h (760 cm^{-1}), in spite of the more planar μ-η^2:η^2-Cu_2O_2 core and longer Cu···Cu distance of **5**.[35] The O–O stretch of **5** is the strongest in the range of 713–765 cm^{-1} for μ-η^2:η^2-Cu_2O_2 complexes, including oxyHc, reported so far.[9] The strong O–O bond may be favorable for release of O_2. Furthermore, it is noted that the O_2^{2-} to Cu^{II} charge-transfer bands at 360 (24700) and 532 nm (1530 M^{-1} cm^{-1}) in the μ-η^2:η^2-Cu_2O_2 complex of H6M4h shift to slightly lower energy in **5** (366 (24000) and 537 nm (2100 M^{-1} cm^{-1})).[35] This indicates that the Cu–O bond in **5** is relatively weak, consistent with the long Cu–O bond of **5** in the solid state. The weak Cu–O bond, the large Cu···Cu distance, and strong O–O bond of **5** are favorable for easy release of O_2. Because of the easy O_2-release, **5** is the best functional model for rever-

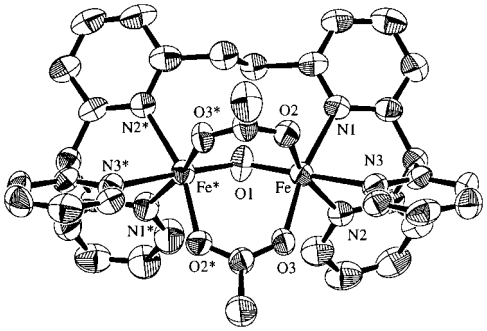

Fig. 6. ORTEP diagram of the cationic portion of $[Fe_2(O)(OAc)_2(hexpy)](ClO_4)_2$ (**7**-$(ClO_4)_2$).

Table 1. Structural Features[74] of Diiron(III) Cores of **7** and the Related Complexes

	7	tripy[a)]	$HB(pz)_3$[b)]	Me_3tacn[c)]
Fe···Fe′/Å	3.142(3)	3.162(2)	3.146(1)	3.12(4)
Fe–O_{oxo}/Å	1.782(5)	1.810(6)	1.788(2)	1.800(3)
			1.780(2)	
Fe–O_{AcO}(av)/Å	2.051(8)	2.015(9)	2.042(9)	2.034(3)
Fe–$N_{cis\ to\ \mu\text{-}oxo}$(av)/Å	2.192(9)	2.165(9)	2.153(3)	2.198(4)
Fe–$N_{trans\ to\ \mu\text{-}oxo}$/Å	2.209(9)	2.32(1)	2.188(3)	2.268(6)
Fe–O–Fe′/deg	123.6(6)	121.7(6)	123.6(1)	119.7(1)

a) tripy: $[Fe_2(O)(OAc)_2(tripy)_2]^{2+}$. b) $HB(pz)_3$: $[Fe_2(O)(OAc)_2(HB(pz)_3)_2]$. c) Me_3tacn: $[Fe_2(O)(OAc)_2(Me_3tacn)_2]^{2+}$.

Table 2. Oxygenation[70] of Various Alkanes Catalyzed by **7**

Substrate	Reaction time/min	Products	Yields/%	Turnover number
Cyclohexane	5	Cyclohexanol	41	164
		Cyclohexanone	17	68
		ε-Caprolactone	12	48
Adamantane	20	1-Adamantanol	41	163
		2-Adamantanol	10	39
		Adamantanone	6	24
Methylcyclohexane	15	1-Methycyclohexanol	26	104
		2-, 3-, and 4-Methycyclohexanols	25	100
		Cyclohexylmethanol	0.5	2
		Methylcyclohexanone	12	48

sible O_2-binding among all μ-η^2:η^2-Cu_2O_2 complexes reported so far.[11] Structural modulation because of the bridgehead methyl groups causes important structural change that facilitates release of O_2. Therefore, these results clearly indicate that structural modulation induced by subtle structural perturbation of the ligand plays essential roles in enhancing the functionality of the metal complex. Structural modulation appears to be essential for developing real functional models.

3. Synthesis, Properties, and Activation of Peroxo–Diiron Complexes

A plausible mechanism for O_2-activation by sMMO is shown in Scheme 2, in which the conversion of intermediate P to active species Q has not been clarified yet. Since it is still difficult to directly observe P and Q due to their instability, a thermally stable μ-1,2-peroxo–diiron(III) complex that can be activated to oxygenate hydrocarbons would be useful as a functional model for elucidating the mechanism for the conversion of P to Q.[12–15] Although a few thermally stable μ-1,2-peroxo–diiron(III) complexes of sterically hindered ligands have been prepared,[13,14] O_2-activation of the thermally stable peroxo complexes has not been fully achieved. The steric hindrance of the ligands that causes the thermal stabilization of the peroxo complexes may inhibit O_2-activation. Thus, a sterically less hindered ligand capable of stabilizing the peroxo–diiron complex may be better for preparing a functional model to study the O_2-activation mechanism of sMMO.

The hexpy ligand forms diiron(III) complexes $[Fe_2(O)(OAc)_2(hexpy)]X_2$ {X = ClO_4 and CF_3SO_3 (**7**-X_2)}.[33,70,71] The crystal structure of **7**-$(ClO_4)_2$ (Fig. 6) showed that the hexpy ligand encapsulates the di-μ-acetato–μ-oxo–diiron(III) core and that there is no large steric hindrance around the diiron core.[33] Typical structural features of the diiron core of **7**-$(ClO_4)_2$ are summarized in Table 1 together with those of diiron(III) complexes of various tridentate ligands, such as di(2-pyridyl)(6-methyl-2-pyridyl)methane (tripy)[74] (see Chart 4), $HB(pz)_3$,[72] and Me_3tacn[73] (see Chart 2). The tripy ligand is a half of the hexpy ligand. The diiron core structure of **7**-$(ClO_4)_2$ is close to those of the azido-met hemerythrin[33] and the diiron complexes of $HB(pz)_3$ and Me_3tacn, rather than that of a diiron(III) complex of the tripy ligand, indicating that the length of the $-CH_2CH_2-$ tether in the hexpy ligand just fits the diiron core size.[74] The diiron complexes of the tridentate ligands are not stable in solution and gradually decompose to the corresponding bis-ligand mononuclear iron complexes.[33] In contrast, **7**-$(ClO_4)_2$ is stable in various solvent systems. Thus, the hexpy ligand specifically stabilizes the diiron core not only thermodynamically but also kinetically in solution.[33,74]

Diiron complex **7** catalyzes alkane oxygenation using *m*-CPBA as an oxidant in $MeCN/CH_2Cl_2$ (1:10, v/v), where various alkanes, for example, cyclohexane, adamantane, and methylcyclohexane, were converted to the corresponding alcohols very efficiently (see Table 2).[70] The turnover number for the oxygenation of cyclohexane exceeded 1000,[70] and it and

product distributions are not affected under either anaerobic or aerobic conditions, indicating that the oxygenation is not a radical chain reaction. The high catalytic activity of **7** may be caused by the stable dinuclear structure and the small steric hindrance around the diiron center. Thus, if a peroxo–diiron complex of the hexpy ligand can be formed, it may be useful as a functional model to study the mechanism for the conversion of P to Q.

A thermally stable peroxo–diiron(III) complex of the hexpy ligand (**8**-CF_3SO_3) was obtained by reacting **7**-$(CF_3SO_3)_2$ with H_2O_2 in the presence of a stoichiometric amount of Et_3N and isolated as a purple solid.[71] Elemental analysis of the isolated solid is consistent with the formula $[Fe_2(O)(O_2)(OAc)(hexpy)](CF_3SO_3)\cdot 5H_2O$.[71] In the FAB-MS spectrum, a parent peak appears at m/z 739 ($[Fe_2(O)(O_2)(OAc)(hexpy)]^+$). The electronic spectrum of **8** in MeCN has two absorption bands (510 ($\varepsilon = 1300\,M^{-1}\,cm^{-1}$) and 605 nm ($\varepsilon = 1310\,M^{-1}\,cm^{-1}$)), similar to the μ-oxo–μ-peroxo–diiron(III) complex of 6-Me_3-tpa ligand (see Chart 2) $[Fe_2(O)(O_2)(6\text{-}Me_3\text{-}tpa)_2](ClO_4)_2$ (**9**) (494 nm ($\varepsilon = 1100\,M^{-1}\,cm^{-1}$), 648 (1200), and 846 (230)).[71,74] The resonance Raman spectrum of **8** obtained with 593 nm excitation has strong bands at 816 and 472 cm^{-1}, which shift to 771 and 455 cm^{-1} by $^{18}O_2$-labeling with $H_2{}^{18}O_2$.[71,74] These ^{18}O-sensitive bands are assigned to the $\nu_{O\text{–}O}$ and the $\nu_{Fe\text{–}O}$ of a bound peroxide, respectively. The Mössbauer spectrum of **8** at 4.2 K shows only a quadrupole doublet with $\Delta E_Q = 1.67(8)\,mm\,s^{-1}$ and $\delta = 0.53(8)\,mm\,s^{-1}$,[71,74] indicating that the high-spin diiron(III) unit is symmetrically bridged by the peroxo ligand. These values are close to $\Delta E_Q = 1.68\,mm\,s^{-1}$ and $\delta = 0.54\,mm\,s^{-1}$ of **9**,[75] and $\Delta E_Q = 1.79\,mm\,s^{-1}$ and $\delta = 0.52\,mm\,s^{-1}$ of a di-μ-benzoato-μ-peroxo–diiron(III) complex with HB(3,5-*i*Pr_2pz)$_3$ ligand (see Chart 2) $[Fe_2(O_2)(OBz)_2\{HB(3,5\text{-}iPr_2pz)_3\}_2]$ (**10**).[27] Cryomagnetic measurements were carried out with a solid sample of **8**, and the exchange-coupling constant (J) was estimated to be $-55\,cm^{-1}$ on the basis of the Heisenberg model [$H = -2JS_1\cdot S_2$].[71] This value is larger than that of **10** ($J = -33\,cm^{-1}$), showing that relatively strong antiferromagnetic interaction operates between the two Fe^{III} ions in **8** because of the μ-oxo bridge.[76] Based on all of the data, **8** has a diiron(III) center triply bridged by an acetato, oxo and peroxo anions. The structure deduced from these data is shown in Scheme 6.

The bridging modes known for triply bridged peroxo–diiron(III) complexes are (1) μ-alkoxo-μ-carboxylato-μ-1,2-peroxo,[50] (2) μ-carboxylato-μ-1,2-peroxo-μ-phenolato,[26] and (3) bis-μ-carboxylato-μ-1,2-peroxo.[27] Thus, the μ-carboxylato-μ-oxo-μ-1,2-peroxo bridge of **8** represents the first example, in which the μ-oxo bridge is involved in the triple bridge. The $\nu_{O\text{–}O}$ value of **8** in the Raman data is notably below the range of 848–900 cm^{-1} reported for μ-1,2-peroxo–diiron(III) complexes.[13] The $\nu_{O\text{–}O}$ value mainly depends on the Fe–O–O angle of peroxo–diiron complex; the $\nu_{O\text{–}O}$ value decreases with decreasing the Fe–O–O angle.[76] Thus, the Raman data indicate that **8** has a smaller Fe–O–O angle than known peroxo–diiron complexes. This is consistent with the structural features of **8**, i.e., short Fe···Fe distance and small Fe–O–O angle, which are expected from the unique triply bridged structure and the encapsulation of the diiron core by the hexpy ligand.[71,74]

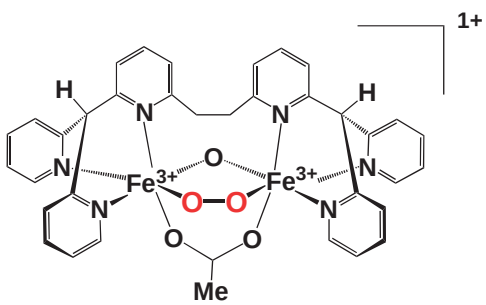

Scheme 6. Proposed chemical structure of peroxo–diiron(III) complex of hexpy ligand.

We found that **8** is thermally stable in spite of no large steric hindrance around the diiron core. The first-order rate constant for spontaneous decomposition of **8** is $k = 2.2 \times 10^{-5}\,s^{-1}$ (half-life $\tau_{1/2} = 8.7$ h) in dry MeCN at 300 K and is independent of the concentration of **8** in the range of 2.0–10.0 $\times$ 10^{-4} M.[71,74] Thus, **8** decomposes unimolecularly. A peroxo–diiron(III) complex of the tripy ligand $[Fe_2(O)(O_2)(OAc)(tripy)_2](ClO_4)$ was prepared to compare the thermal stability.[71,74] The half-life time $\tau_{1/2}$ values, 10 min, of the peroxo–diiron complex with the tripy ligand at 263 K and 7.2 min of **9**[75] at 243 K are much smaller than 8.7 h of **8** at 300 K. These kinetic data demonstrate that the hexpy ligand specifically stabilizes the peroxo–diiron core.

Product analysis and kinetic studies provide some insight into the mechanism for the spontaneous decomposition of **8**.[74] The only detectable product for the spontaneous decomposition is the precursor **7**. After demetallation of the product, the hexpy ligand is recovered quantitatively. In the presence of an excess amount of cyclohexane as a substrate, oxygenation of cyclohexane was not observed at all. Moreover, we measured the spontaneous decomposition rate of **8** in d_3-MeCN, and the k_H/k_D value is 0.9, which is not consistent with a first-order kinetic isotope effect.[74] Thus, H-abstraction from MeCN is not involved in the rate-determining step of the spontaneous decomposition of **8**. These results indicate that O_2-activation does not occur during the spontaneous decomposition. This is further supported by detailed kinetic studies for the spontaneous decomposition of **8** in various solvent systems.[74] Kinetic data obtained in polar solvent systems H_2O/MeCN ($[H_2O] = 0.28$–2.22 M) is shown in Fig. 7. The rate constants increase with an increase in the concentration of H_2O, with a y-axis intercept of $2.2 \times 10^{-5}\,s^{-1}$. This clearly shows that **8** decomposes in the absence of H_2O, and it is accelerated by the addition of H_2O. Thus, both MeCN and H_2O cause the decomposition of **8**. The rate constant, $8.0 \times 10^{-5}\,s^{-1}$, in H_2O/MeCN (1:9, v/v) is nearly four-fold larger than that in dry MeCN. This is because the nucleophilicity of H_2O is higher than that of MeCN. The rate dependence of H_2O is not linear and seems to reflect a second-order dependence (see Fig. 8). The hydrogen bond of another H_2O molecule to the peroxo moiety of **8** may be involved in the acceleration. The spontaneous decomposition of **8** was retarded in a non-polar solvent system CH_2Cl_2/MeCN (3:1, v/v), and $\tau_{1/2}$ at 300 K was 20.3 h.[74] This value is 2.3-times larger than 8.7 h, which is the $\tau_{1/2}$ observed in dry MeCN. The nucleophilicity of MeCN

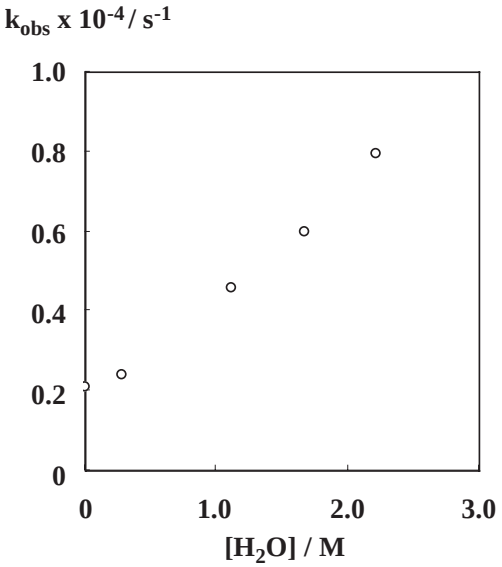

Fig. 7. First-order rate constants at various concentrations of H_2O, [**8**] = 3.0×10^{-4} M, [H_2O] = (4×10^{-3}–2.22) M in MeCN at 300 K.

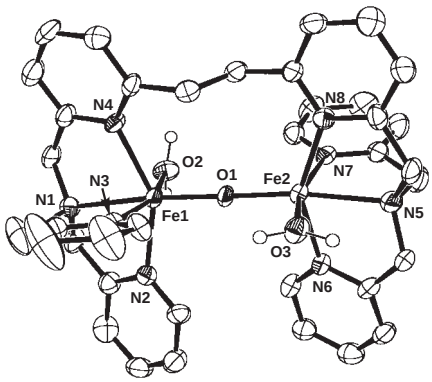

Fig. 8. ORTEP diagram of the cationic portion of [Fe_2(O)-(H_2O)$_2$(6-hpa)](ClO_4)$_4$ (**11**).

may be reduced in the non-polar solvent system. All of these results are consistent with nucleophilic substitution of the bound peroxo with polar solvent molecules. Therefore, it is concluded that the bound peroxo is not activated in the spontaneous decomposition of **8**.

Activation of **8** was examined under various conditions.[71] Upon addition of $HClO_4$ or *m*-ClC_6H_4COCl (*m*-CBC), **8** decomposed more rapidly ($k_{obs} = 8.0 \times 10^{-2}$ s^{-1} for **8** (1.0×10^{-3} M)/*m*-CBC (3.0×10^{-2} M) in CH_2Cl_2/MeCN (6:2, v/v) at 273 K), but in the presence of alkane as a substrate, oxygenation of alkane was not observed.[71] In the presence of DMF, the decomposition of **8** by addition of *m*-CBC is 20-times faster ($k_{obs} = 1.6$ s^{-1} for **8** (1.0×10^{-3} M)/*m*-CBC (3.0×10^{-2} M) in CH_2Cl_2/MeCN/DMF (6:2:1, v/v) at 273 K), and cyclohexane was oxygenated to cyclohexanol and cyclohexanone. Thus, the peroxo moiety of **8** can be activated in the presence of both acid chloride and DMF to oxygenate external hydrocarbons.[71] The reason why DMF is necessary for the activation of **8** is that acid chloride itself is not active enough to acylate the peroxo oxygen of **8**, and acylation occurs via activation by

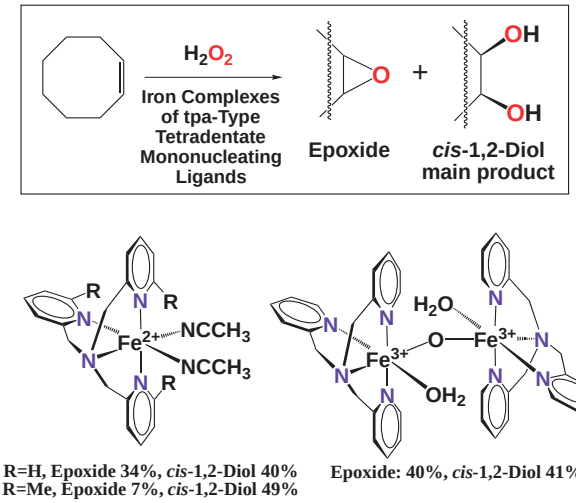

Scheme 7. Oxygenation of alkenes with H_2O_2 catalyzed by iron complexes of tpa-type tetradentate mononucleating ligands.[81]

DMF. The yields of the C–H oxygenation products, however, are in a range of 6–29% based on the peroxo complex **8** used. These values are not high enough, indicating that it is not easy to activate such a stable peroxo complex. Therefore, a peroxo–diiron complex that can be more easily activated is necessary as an functional model of sMMO to elucidate the mechanism for conversion of the peroxo intermediate P to the active species Q in the O_2-activation by sMMO.

4. Predominant Epoxidation via O_2-Activation of a Peroxo–Diiron(III) Complex

As shown above, the activation of the thermally stable peroxo complex **8** is difficult. On the other hand, diiron complexes of tris(2-pyridylmethyl)amine (tpa, see Chart 2) and related ligands are known as an effective sMMO models.[77–79] This type of tetradentate ligands, however, are not dinucleating ligands, and do not specifically stabilize the diiron strucutre in solution.[80] The resulting complexes, therefore, potentially form both mono- and diiron complexes in solution with varied reactivity, depending on the structures.[81–84] Iron complexes of tpa derivatives catalyze alkene oxidation with H_2O_2 to give 1,2-*cis*-diol and epoxide (see Scheme 7),[81] where Rieske dioxygenase-type monoiron acive species have been proposed.[81–83] On the other hand, with the iron complex of *N*,*N*′-dimethyl-*N*,*N*′-bis(2-pyridylmethyl)ethane-1,2-diamine (mep, see Chart 2), a tetradentate ligand similar to tpa, predominant epoxidation was observed, and an sMMO type diiron species was proposed.[84] Therefore, a tpa-containing dinucleating ligand capable of stabilizing a diiron core in solution would be useful for an effective sMMO model.

We synthesized 1,2-bis[2-(bis(2-pyridylmethyl)aminomethyl)-6-pyridyl]ethane (6-hpa, see Chart 3) as a new bis-tpa dinucleating ligand.[36] The 6-hpa ligand forms diiron(III) and diiron(II) complexes [Fe_2(O)(OH_2)$_2$(6-hpa)](ClO_4)$_4$ (**11**) and [Fe_2(TfO)$_4$(6-hpa)] (**12**), respectively.[36] Crystal structure of **11** is shown in Fig. 8. The crystal structure of the diiron core of **11** is very similar to that of a diiron(III) complex of tpa, [Fe_2(O)(OH_2)$_2$(tpa)$_2$](ClO_4)$_3$ (**13**).[85] The bond distances and

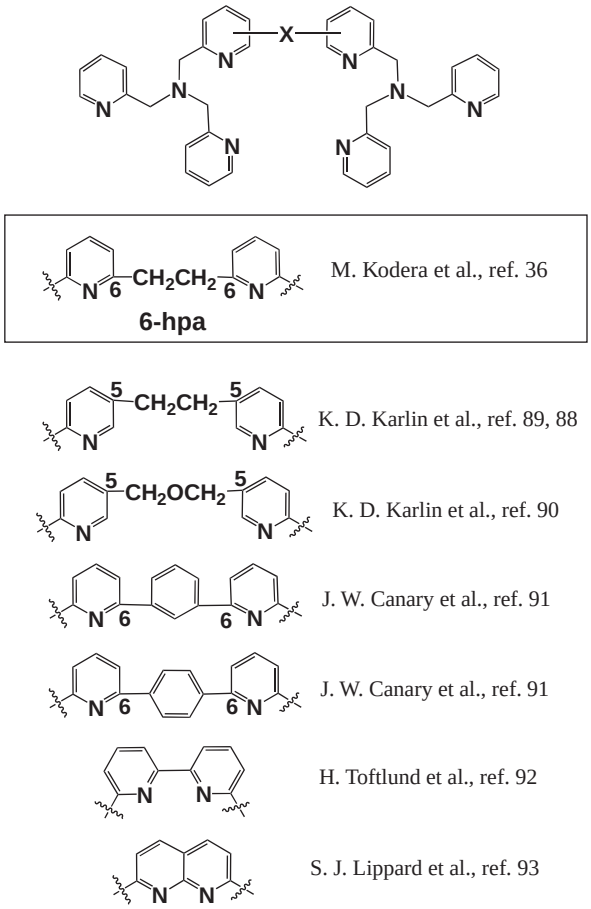

Chart 5.

angles of the diiron cores are almost equivalent between **11** and **13**, showing that 6-hpa stabilizes the diiron core without distortion. ESI-MS spectrum of **11** has a major peak at m/z 1033, corresponding to $\{[Fe_2(O)(OH_2)_2(6\text{-hpa})](ClO_4)_3\}^+$, but **13** gave two major peaks at m/z 362 and 445 due to monoiron complexes and two minor peaks at m/z 923 and 1007 due to diiron complexes, clearly showing that 6-hpa specifically stabilizes the diiron core in solution.[36] Although various bis-tpa type ligands shown in Chart 5 were reported, 6-hpa seems the best ligand to obtain diiron complexes as a functional model of sMMO because it specifically stabilizes the dinuclear structure and forms a flexible structure as shown by the undistorted diiron core of **11**.

Efficient and predominant epoxidation of alkenes with H_2O_2 catalyzed by **11** was attained.[36] Cyclooctene was converted to an epoxide and 1,2-*cis*-diol in 75 and 2% yields, respectively. The turnover number of **11** exceeded one hundred. For other alkenes, the 1,2-*cis*-diol was not detected at all. From *trans*-β-methylstyrene, the *trans*-epoxide was obtained in 91% yield based on the H_2O_2 used. Given the large turnover number and high epoxide yield, it can be said that **11** is an effective sMMO model. Epoxidation was not stereospecific since *cis*- and *trans*-epoxides were obtained from *cis*-β-methylstyrene with RC value of 63%,[86] indicating that the first step in the epoxidation may be a one-electron oxidation of the alkene by an active species and that the cation radical generated undergoes a *cis* to *trans* configuration change. Since 6-hpa stabilizes the diiron

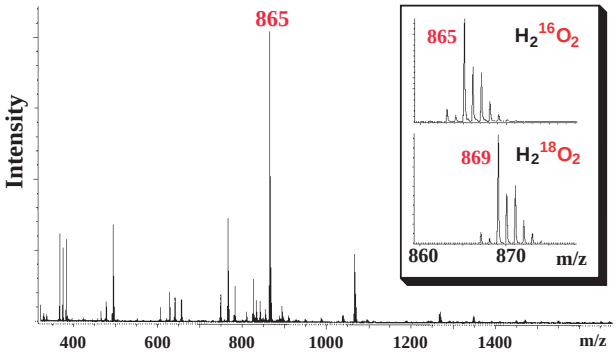

Fig. 9. CSI-MS spectrum of peroxo–diiron(III) complex with 6-hpa (**14**) observed at −40 °C in MeCN. Inset: Isotope patterns assignable to $\{[Fe_2(O)(^{16}O_2)(6\text{-hpa})](ClO_4)\}^+$ and $\{[Fe_2(O)(^{18}O_2)(6\text{-hpa})](ClO_4)\}^+$.

core of **11** in solution, the active species generated from **11** must be a dinuclear complex relevant to sMMO. Interestingly, however, when the diiron(II) complex, which does not have bridging oxo or hydroxo ligands, was used as a catalyst for the oxygenation of cyclooctene, the 1,2-*cis*-diol was main product. The diiron(II) complex of 6-hpa (**12**) gave an epoxide/*cis*-1,2-diol products ratio of 0.15/0.85, when 1 equiv of H_2O_2 was added. When the amount of H_2O_2 was increased, the yield of epoxide increased and that of *cis*-1,2-diol decreased as follows: the epoxide/*cis*-1,2-diol ratios were 0.26/0.74, 0.53/0.47, and 0.64/0.36 for 2, 5, and 10 equiv of H_2O_2 added, respectively. In other words, **12** mainly produces *cis*-1,2-diol, and **11**, which is generated by the oxidation of **12** with H_2O_2, mainly produces epoxide. This indicated that the μ-oxo bridge in **11** plays an essential role in the sMMO-type reactivity.

Addition of 2.0 equiv of H_2O_2 to a solution of **11** in MeCN at −40 °C generated a green species **14** that exhibits electronic absorption bands at 490 nm ($\varepsilon = 1130\,M^{-1}\,cm^{-1}$), 670 (1060), and 882 (sh, 370), similar to those reported for the peroxo–diiron(III) complex of a sterically hindered tpa-type ligand, tris(6-methyl-2-pyridylmethyl)amine (6-Me$_3$-tpa, see Chart 2), (**9**).[75] In CSI MS spectrum of **14**, shown in Fig. 9, a parent peak was observed at m/z 865, corresponding to $\{[Fe_2(O)(O_2)(6\text{-hpa})](ClO_4)\}^+$, as the strongest peak. Upon addition of $H_2{}^{18}O_2$ instead of $H_2{}^{16}O_2$, the mass number of the ion increased by 4 units (see Fig. 9). These show that **14** is the peroxo–diiron(III) complex $[Fe_2(O)(O_2)(6\text{-hpa})](ClO_4)_2$, similar to **9**. The half-life time of **14** in MeCN at 243 K is $\tau_{1/2} = 7.2$ min, equivalent to the half-life time of **9** (7 min) under the same conditions.[75] When *trans*-β-methylstyrene was added to the solution of **14** at −40 °C, the decay rate of **14** did not accelerate, indicating that **14** is not a direct oxidant for the epoxidation. Thus, the peroxo–diiron(III) complex **14** is an intermediate and must be converted to an active species in the catalytic epoxidation.

Isotope-labeling experiments using *trans*-β-methylstyrene as a substrate were carried out with $H_2{}^{18}O_2$ and μ-^{18}O-**11** under Ar to gain insight into the O_2-activation mechanism.[36] Upon addition of 10 equiv of $H_2{}^{18}O_2$ to **11**, ^{18}O was incorporated into 94% of the epoxide. Upon addition of 1 or 3 equiv of $H_2{}^{16}O_2$ to μ-^{18}O-**11**, ^{18}O was incorporated into the epoxide 31 or 17%, respectively. Thus, in addition to $H_2{}^{18}O_2$, μ-^{18}O is in-

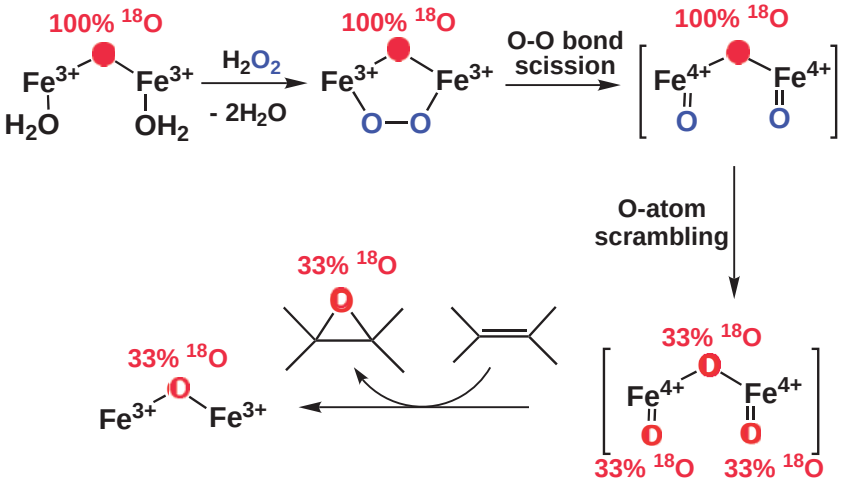

Scheme 8. Incorporation of μ-^{18}O-atom to epoxide via homolytic O–O bond scission of the peroxo intermediate and scrambling of three O-atoms of the active species.

corporated into the epoxide. This could be explained by assuming that a dioxo–μ-oxo–diiron(IV) complex is generated from **14** as an active species via homolytic scission of the O–O bond and scrambling of the three O-atoms in the active species. Accordingly, as shown in Scheme 8, with $H_2{}^{16}O_2$ (1 equiv)/μ-^{18}O-**11**, 33% of each oxo in the active species was ^{18}O-labeled, and thus, the theoretical yield of the ^{18}O-epoxide is 33%. Similarly, with $H_2{}^{16}O_2$ (3 equiv)/μ-^{18}O-**11** or $H_2{}^{18}O_2$ (10 equiv)/**11**, the yield of ^{18}O-epoxide was estimated to be 16 or 95%, respectively. The theoretical values 33, 16, and 95% agree with the experimental results 31, 17, and 94%, respectively. Further experiments using an excess amount of $H_2{}^{18}O$ or under $^{18}O_2$ revealed unique reactivity of the active species. With $H_2{}^{18}O/H_2{}^{16}O_2$/**11** (1000/10/1), only 1.5% of the epoxide was ^{18}O-labeled, showing that O-atom exchange between the active species and H_2O is much slower than O-atom transfer from the active species to the alkene.[87] When the reaction was carried out with $H_2{}^{16}O_2$ (10 equiv)/**11** under $^{18}O_2$, 5% of the epoxide was ^{18}O-labeled. This suggests that a one-electron oxidation of the alkene by the active species occurs, forming a radical cation and a diiron(III)(IV) species since ^{18}O-labelling from $^{18}O_2$ must occur by autoxidation of the radical cation. The remaining 95% of unlabeled epoxide could be accounted for O-atom transfer from the resultant diiron(III)(IV) species to the radical cation. On the basis of all these results, we propose a mechanism for epoxidation via O_2-activation by the diiron complex of 6-hpa, Scheme 9.

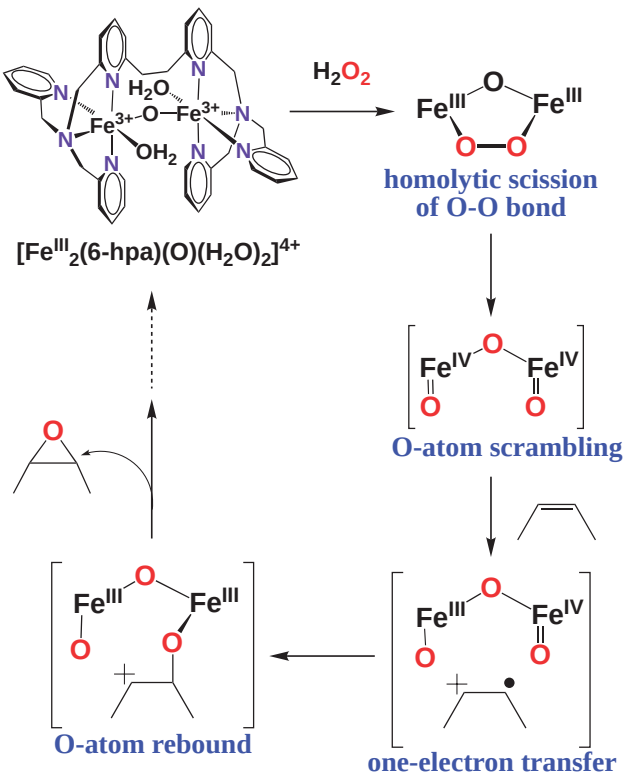

Scheme 9. Plausible mechanism for catalytic epoxidation via O_2-activation by diiron complex of 6-hpa.

Conclusion

We have synthesized various hexapyridine ligands to stabilize potentially reactive peroxo–dimetal complexes and found that stabilization of the dinuclear structure, optimization of the metal–metal distance, encapsulation of the dimetal core are the key aspects for stabilizing the peroxo–dimetal complexes. The hexpy ligand can thermally stabilize the peroxo–diiron(III) complex. On the other hand, the sterically hindered hexapyridine ligand (H6M4h), in which four methyl groups are introduced at the 6-py positions of the hexpy ligand for the purpose of steric hindrance, was developed to obtain a thermally stable μ-η^2:η^2-peroxo–dicopper(II) complex. We attained reversible O_2-binding with the μ-η^2:η^2-peroxo–dicopper(II) complex of H6M4h at room temperature. At this stage, we reached the first goal, i.e., the stabilization of reactive peroxo–dimetal complexes. In the next step, we need to enhance the functionality of the peroxo–dimetal complexes. In the case of copper complexes, our goal was to improve the reversible O_2-binding to obtain a better functional model of hemocyanin. We found that the copper complexes of sterically hindered tripyridine ligand, tris(6-methyl-2-pyridyl)methane, can be structurally modulated by methylation at the bridgehead position. This is applied to the sterically hindered hexapyridine ligand, where the

H6M4h ligand was converted to the M6M4h analogue. Reversible O_2-binding is greatly improved using the μ-η^2:η^2-peroxo–dicopper(II) complex of M6M4h ligand, which is the best functional model of hemocyanin at moment. In the case of iron complexes, our focus was the activation of the peroxo–diiron(III) complex as a functional model of sMMO, but the peroxo–diiron(III) complex of hexpy ligand is thermally too stable to be activated. In other words, a ligand that specifically stabilizes the peroxo complex is not suitable for studying the mechanism of conversion of the peroxo complex to the active species. In contrast, the 6-hpa ligand, which has two tpa moieties connected at the 6-py positions with the $-CH_2CH_2-$ tether, is a promising ligand for preparing a functional model of sMMO. The diiron complex of 6-hpa ligand efficiently and predominantly catalyzes the epoxidation of various alkenes via O_2-activation of the peroxo–diiron(III) intermediate. The 6-hpa ligand may stabilize both the peroxo–diiron(III) complex and the active species which epoxidizes various alkenes. This is probably caused by the flexible structure of 6-hpa. The flexibility of the dinucleating ligand may be one of the most important aspects for achieving O_2-activation with the peroxo complex to form the active species.

References

1 *Oxygenases and Model Systems*, ed. by T. Funabiki, Kluwer Academic Publishers, Dordrecht, **1997**.

2 R. H. Holm, E. I. Solomon, *Chem. Rev.* **2004**, *104*, 347.

3 *Advances in Catalytic Activation of Dioxygen by Metal Complexes*, ed. by L. I. Simándi, Kluwer Academic Publishers, Dordrecht, Boston, London, **2003**.

4 *Handbook of Metalloproteins*, ed. by A. Messerschmidt, R. Huber, T. Poulos, K. Wieghardt, John Wiley & Sons, Chichester, 2001, Vols. 1 and 2.

5 *Handbook of Metalloproteins*, ed. by I. Bertini, R. Huber, A. Sigel, H. Sigel, Marvel Dekker, New York, **2001**.

6 K. D. Karlin, *Science* **1993**, *261*, 710.

7 N. Kitajima, *Adv. Inorg. Chem.* **1992**, *39*, 1.

8 S. Itoh, S. Fukuzumi, *Bull. Chem. Soc. Jpn.* **2002**, *75*, 2081.

9 L. M. Mirica, T. D. P. Stack, *Chem. Rev.* **2004**, *104*, 1013.

10 E. A. Lewis, W. B. Tolman, *Chem. Rev.* **2004**, *104*, 1047.

11 P. Gamez, I. A. Koval, J. Reedijk, *Dalton Trans.* **2004**, 4079.

12 M. Costas, M. P. Mehn, M. P. Jensen, L. Que, Jr., *Chem. Rev.* **2004**, *104*, 939.

13 E. Y. Tshuva, S. J. Lippard, *Chem. Rev.* **2004**, *104*, 987.

14 S. V. Kryatov, E. V. Rybak-Akimova, S. Schindler, *Chem. Rev.* **2005**, *105*, 2175.

15 X. Shan, L. Que, Jr., *J. Inorg. Biochem.* **2006**, *100*, 421.

16 K. A. Magnus, H. Ton-That, J. E. Carpenter, *Chem. Rev.* **1994**, *94*, 727.

17 A. L. Feig, S. J. Lippard, *Chem. Rev.* **1994**, *94*, 759.

18 M. Kodera, K. Kano, T. Funabiki, *Oxygenases and Model Systems*, ed. by T. Funabiki, Kluwer Academic Publishers, Dordrecht, **1997**, pp. 283.

19 B. J. Wallar, J. D. Lipscomb, *Chem. Rev.* **1996**, *96*, 2625.

20 M. Merkx, D. A. Kopp, M. H. Sazinsky, J. L. Blazyk, J. Müller, S. J. Lippard, *Angew. Chem., Int. Ed.* **2001**, *40*, 2782.

21 S.-K. Lee, J. C. Nesheim, J. D. Lipscomb, *J. Biol. Chem.* **1993**, *268*, 21569.

22 S.-K. Lee, B. G. Fox, W. A. Froland, J. D. Lipscomb, E. Münck, *J. Am. Chem. Soc.* **1993**, *115*, 6450.

23 K. E. Liu, D. Wang, B. H. Huynh, D. E. Edmondson, A. Salifoglou, S. J. Lippard, *J. Am. Chem. Soc.* **1994**, *116*, 7465.

24 K. E. Liu, A. M. Valentine, D. Qiu, D. E. Edmondson, E. H. Appelman, T. G. Spiro, S. J. Lippard, *J. Am. Chem. Soc.* **1995**, *117*, 4997.

25 L. Shu, J. C. Nesheim, K. Kauffmann, E. Münck, J. D. Lipscomb, L. Que, Jr., *Science* **1997**, *275*, 515.

26 T. Ookubo, H. Sugimoto, T. Nagayama, H. Masuda, T. Sato, K. Tanaka, Y. Maeda, H. Okawa, Y. Hayashi, A. Uehara, M. Suzuki, *J. Am. Chem. Soc.* **1996**, *118*, 701.

27 K. Kim, S. J. Lippard, *J. Am. Chem. Soc.* **1996**, *118*, 4914.

28 Y. Dong, S. Yan, V. G. Young, L. Que, Jr., *Angew. Chem., Int. Ed. Engl.* **1996**, *35*, 618.

29 L. Que, Jr., Y. Dong, *Acc. Chem. Res.* **1996**, *29*, 190.

30 C. A. Grapperhaus, B. Mienert, E. Bill, T. Weyhermüller, K. Wieghardt, *Inorg. Chem.* **2000**, *39*, 5306.

31 J.-U. Rohde, J.-H. In, M. H. Lim, W. W. Brennessel, M. R. Bukowski, A. Stubna, E. Münck, W. Nam, L. Que, Jr., *Science* **2003**, *299*, 1037.

32 M. Costas, M. P. Mehn, M. P. Jensen, L. Que, Jr., *Chem. Rev.* **2004**, *104*, 939.

33 M. Kodera, H. Shimakoshi, M. Nishimura, H. Okawa, S. Iijima, K. Kano, *Inorg. Chem.* **1996**, *35*, 4967.

34 M. Kodera, K. Katayama, Y. Tachi, K. Kano, S. Hirota, S. Fujinami, M. Suzuki, *J. Am. Chem. Soc.* **1999**, *121*, 11006.

35 M. Kodera, Y. Kajita, Y. Tachi, K. Katayama, K. Kano, S. Hirota, S. Fujinami, M. Suzuki, *Angew. Chem., Int. Ed.* **2004**, *43*, 334.

36 M. Kodera, M. Itoh, K. Kano, S. Hirota, T. Funabiki, M. Reglier, *Angew. Chem., Int. Ed.* **2005**, *44*, 7104.

37 M. Itoh, J. Nakazawa, K. Maeda, K. Kano, T. Mizutani, M. Kodera, *Inorg. Chem.* **2005**, *44*, 691.

38 Z. Hu, G. N. George, S. M. Gorun, *Inorg. Chem.* **2001**, *40*, 4812.

39 W. E. Lynch, D. M. Kurtz, S. K. Wang, R. A. Scott, *J. Am. Chem. Soc.* **1994**, *116*, 11030.

40 T. N. Sorrell, W. E. Allen, P. S. White, *Inorg. Chem.* **1995**, *34*, 952.

41 H. V. Obias, Y. Lin, N. N. Murthy, E. Pidcock, E. I. Solomon, M. Ralle, N. J. Blackburn, Y. M. Neuhold, A. D. Zuberbühler, K. D. Karlin, *J. Am. Chem. Soc.* **1998**, *120*, 12960.

42 S. Itoh, H. Nakao, L. M. Berreau, T. Kondo, M. Komatsu, S. Fukuzumi, *J. Am. Chem. Soc.* **1998**, *120*, 2890.

43 S. Itoh, H. Kumei, M. Taki, S. Nagatomo, T. Kitagawa, S. Fukuzumi, *J. Am. Chem. Soc.* **2001**, *123*, 6708.

44 K. D. Karlin, M. S. Haka, R. W. Cruse, Y. Gultneh, *J. Am. Chem. Soc.* **1985**, *107*, 5828.

45 A. L. Gavrilova, B. Bosnich, *Chem. Rev.* **2004**, *104*, 349.

46 M. Kodera, Y. Tachi, S. Hirota, K. Katayama, H. Shimakoshi, K. Kano, K. Fujisawa, Y. Moro-oka, Y. Naruta, T. Kitagawa, *Chem. Lett.* **1998**, 389.

47 M. Kodera, H. Shimakoshi, Y. Tachi, K. Katayama, K. Kano, *Chem. Lett.* **1998**, 441.

48 N. Kitajima, K. Fujisawa, C. Fujimoto, Y. Moro-oka, S. Hashimoto, T. Kitagawa, K. Toriumi, K. Tatsumi, A. Nakamura, *J. Am. Chem. Soc.* **1992**, *114*, 1277.

49 M. Kodera, N. Terasako, T. Kita, Y. Tachi, K. Kano, M. Yamazaki, M. Koikawa, T. Tokii, *Inorg. Chem.* **1997**, *36*, 3861.

50 Y. Hayashi, T. Kayatani, H. Sugimoto, M. Suzuki, K. Inomata, A. Uehara, Y. Mizutani, T. Kitagawa, Y. Maeda, *J. Am. Chem. Soc.* **1995**, *117*, 11220.

51 N. Kitajima, T. Koda, S. Hashimoto, T. Kitagawa, Y. Moro-oka, *J. Am. Chem. Soc.* **1991**, *113*, 5664.
52 Z. Hu, R. D. Williams, D. Tran, T. G. Spiro, S. M. Gorun, *J. Am. Chem. Soc.* **2000**, *122*, 3556.
53 Z. Tyeklár, K. D. Karlin, *Acc. Chem. Res.* **1989**, *22*, 241.
54 P. L. Holland, W. B. Tolman, *Coord. Chem. Rev.* **1999**, *190–192*, 855.
55 S. Schindler, *Eur. J. Inorg. Chem.* **2000**, 2311.
56 K. D. Karlin, J. C. Hayes, S. Juen, J. P. Hutchinson, J. Zubieta, *Inorg. Chem.* **1982**, *21*, 4106.
57 R. R. Jacobson, Z. Tyeklar, A. Farooq, K. D. Karlin, S. Liu, J. Zubieta, *J. Am. Chem. Soc.* **1988**, *110*, 3690.
58 P. P. Paul, Z. Tyeklar, R. R. Jacobson, K. D. Karlin, *J. Am. Chem. Soc.* **1991**, *113*, 5322.
59 K. D. Karlin, S. Kaderli, A. D. Zuberbühler, *Acc. Chem. Res.* **1997**, *30*, 139.
60 M. Schatz, M. Becker, F. Thaler, F. Hampel, S. Schindler, R. R. Jacobson, Z. Tyeklár, N. N. Murthy, P. Ghosh, Q. Chen, J. Zubieta, K. D. Karlin, *Inorg. Chem.* **2001**, *40*, 2312.
61 H. Nagao, N. Komeda, M. Mukaida, M. Suzuki, K. Tanaka, *Inorg. Chem.* **1996**, *35*, 6809.
62 T. Osako, Y. Tachi, M. Taki, S. Fukuzumi, S. Itoh, *Inorg. Chem.* **2001**, *40*, 6604.
63 M. Taki, S. Teramae, S. Nagatomo, Y. Tachi, T. Kitagawa, S. Itoh, S. Fukuzumi, *J. Am. Chem. Soc.* **2002**, *124*, 6367.
64 S. Trofimenko, *Chem. Rev.* **1993**, *93*, 943.
65 S. M. Carrier, C. E. Ruggiero, R. P. Houser, W. B. Tolman, *Inorg. Chem.* **1993**, *32*, 4889.
66 K. Fujisawa, M. Tanaka, Y. Moro-oka, N. Kitajima, *J. Am. Chem. Soc.* **1994**, *116*, 12079.
67 M. Kodera, Y. Kajita, Y. Tachi, K. Kano, *Inorg. Chem.* **2003**, *42*, 1193.
68 M. Kodera, Y. Tachi, T. Kita, H. Kobushi, Y. Sumi, K. Kano, M. Shiro, M. Koikawa, T. Tokii, M. Ohba, H. Okawa, *Inorg. Chem.* **2000**, *39*, 226.
69 E. Pidcock, H. V. Obias, M. Abe, H.-C. Liang, K. D. Karlin, E. I. Solomon, *J. Am. Chem. Soc.* **1999**, *121*, 1299.
70 M. Kodera, H. Shimakoshi, K. Kano, *Chem. Commun.* **1996**, 1737.
71 M. Kodera, Y. Taniike, M. Itoh, Y. Tanahashi, H. Shimakoshi, K. Kano, S. Hirota, S. Iijima, M. Ohba, H. Okawa, *Inorg. Chem.* **2001**, *40*, 4821.
72 W. H. Armstrong, A. Spool, G. C. Papaefthymiou, R. B. Frankel, S. J. Lippard, *J. Am. Chem. Soc.* **1984**, *106*, 3653.
73 J.-A. R. Hartman, R. L. Rardin, P. Chaudhuri, K. Pohl, K. Wieghardt, B. Nuber, J. Weiss, G. C. Papaefthymiou, R. B. Frankel, S. J. Lippard, *J. Am. Chem. Soc.* **1987**, *109*, 7387.
74 M. Kodera, M. Itoh, K. Kano, T. Funabiki, *Bull. Chem. Soc. Jpn.* **2006**, *79*, 252.
75 Y. Dong, Y. Zang, L. Shu, E. C. Wilkinson, L. Que, Jr., *J. Am. Chem. Soc.* **1997**, *119*, 12683.
76 T. C. Brunold, N. Tamura, N. Kitajima, Y. Moro-oka, E. I. Solomon, *J. Am. Chem. Soc.* **1998**, *120*, 5674.
77 Y. Dong, H. Fujii, M. P. Hendrich, R. A. Leising, G. Pan, C. R. Randall, E. C. Wilkinson, Y. Zang, L. Que, Jr., B. G. Fox, K. Kauffman, E. Münck, *J. Am. Chem. Soc.* **1995**, *117*, 2778.
78 C. Kim, Y. Dong, L. Que, Jr., *J. Am. Chem. Soc.* **1997**, *119*, 3635.
79 H.-F. Hsu, Y. Dong, L. Shu, V. G. Young, Jr., L. Que, Jr., *J. Am. Chem. Soc.* **1999**, *121*, 5230.
80 J. Kim, Y. Dong, E. Larka, L. Que, Jr., *Inorg. Chem.* **1996**, *35*, 2369.
81 K. Chen, M. Costas, J. Kim, A. K. Tipton, L. Que, Jr., *J. Am. Chem. Soc.* **2002**, *124*, 3026.
82 M. Costas, L. Que, Jr., *Angew. Chem., Int. Ed.* **2002**, *41*, 2179.
83 M. Fujita, M. Costas, L. Que, Jr., *J. Am. Chem. Soc.* **2003**, *125*, 9912.
84 M. C. White, A. G. Doyle, E. N. Jacobsen, *J. Am. Chem. Soc.* **2001**, *123*, 7194.
85 B. R. Whittlesey, Z. Pang, R. A. Holwerda, *Inorg. Chim. Acta* **1999**, *284*, 124.
86 RC(%) of epoxide $= 100 \times (cis - trans)/(cis + trans)$.
87 M. S. Seo, J.-H. In, S. O. Kim, N. Y. Oh, J. Hong, J. Kim, L. Que, Jr., W. Nam, *Angew. Chem., Int. Ed.* **2004**, *43*, 2417.
88 N. Wei, D.-H. Lee, N. N. Merthy, Z. Tyeklár, K. D. Karlin, S. Kaderli, B. Jung, A. D. Zuberbühler, *Inorg. Chem.* **1994**, *33*, 4625.
89 D.-H. Lee, N. Wei, N. N. Merthy, Z. Tyeklár, K. D. Karlin, S. Kaderli, B. Jung, A. D. Zuberbühler, *J. Am. Chem. Soc.* **1995**, *117*, 12498.
90 K. D. Karlin, D.-H. Lee, S. Kaderli, A. D. Zuberbühler, *Chem. Commun.* **1997**, 475.
91 L. Zhu, O. Santos, C. W. Koo, M. Rybstein, L. Pape, J. W. Canary, *Inorg. Chem.* **2003**, *42*, 7912.
92 A. Døssing, A. Hazell, H. Toftlund, *Acta Chem. Scand.* **1996**, *50*, 95.
93 C. He, S. J. Lippard, *Inorg. Chem.* **2001**, *40*, 1414.

Masahito Kodera was born in 1960 in Saitama, Japan. He received his Doctor's degree in engineering under the supervision of Professor Iwao Tabushi from Kyoto University in 1987. He was also received Research Fellowships for Young Scientists during 1986–1987 from Japan Society for the Promotion of Science (JSPS). He was appointed Assistant Professor at the Institute for Molecular Science in 1987, and moved to the Faculty of Science at Kyushu University, where he worked on the coordination chemistry. During that period, he spent one year and two months (1990–1991) as a postdoctoral fellow in Professor Alan R. Battersby's group at the Cambridge University, where he learned the chemistry of biosynthesis of vitamin B_{12}. In 1993, he moved to Doshisha University and was promoted to full professor in 2001. His research interest is centered on mechanisms involving metalloproteins and the development of their functional models and bioinspired molecules.

Koji Kano was born in 1944 in Kyoto and graduated from Doshisha University in 1972 with a doctor of engineering degree. After serving as a research assistant and a lecturer at Kyushu University, he was appointed as an associate professor at Kyushu University where he worked with Professors Taku Matsuo and Teiichiro Ogawa. In 1983, he moved to Doshisha University and was promoted to full professor of the Faculty of Engineering in 1985. His current research interest is the supramolecular chemistry involving both water-soluble prophyrins and modified cyclodextrins and also the chemistry of metalloprotein models. He received the Society of Cyclodextrin, Japan Award in 2004.